NASA/TM—2018-219940

Low Power Radioisotope Conversion Technology and Performance Summary

Anthony J. Colozza
Vantage Partners, LLC, Brook Park, Ohio

Robert L. Cataldo
Glenn Research Center, Cleveland, Ohio

October 2018

NASA STI Program . . . in Profile

Since its founding, NASA has been dedicated to the advancement of aeronautics and space science. The NASA Scientific and Technical Information (STI) Program plays a key part in helping NASA maintain this important role.

The NASA STI Program operates under the auspices of the Agency Chief Information Officer. It collects, organizes, provides for archiving, and disseminates NASA's STI. The NASA STI Program provides access to the NASA Technical Report Server—Registered (NTRS Reg) and NASA Technical Report Server—Public (NTRS) thus providing one of the largest collections of aeronautical and space science STI in the world. Results are published in both non-NASA channels and by NASA in the NASA STI Report Series, which includes the following report types:

- TECHNICAL PUBLICATION. Reports of completed research or a major significant phase of research that present the results of NASA programs and include extensive data or theoretical analysis. Includes compilations of significant scientific and technical data and information deemed to be of continuing reference value. NASA counter-part of peer-reviewed formal professional papers, but has less stringent limitations on manuscript length and extent of graphic presentations.

- TECHNICAL MEMORANDUM. Scientific and technical findings that are preliminary or of specialized interest, e.g., "quick-release" reports, working papers, and bibliographies that contain minimal annotation. Does not contain extensive analysis.

- CONTRACTOR REPORT. Scientific and technical findings by NASA-sponsored contractors and grantees.

- CONFERENCE PUBLICATION. Collected papers from scientific and technical conferences, symposia, seminars, or other meetings sponsored or co-sponsored by NASA.

- SPECIAL PUBLICATION. Scientific, technical, or historical information from NASA programs, projects, and missions, often concerned with subjects having substantial public interest.

- TECHNICAL TRANSLATION. English-language translations of foreign scientific and technical material pertinent to NASA's mission.

For more information about the NASA STI program, see the following:

- Access the NASA STI program home page at http://www.sti.nasa.gov

- E-mail your question to help@sti.nasa.gov

- Fax your question to the NASA STI Information Desk at 757-864-6500

- Telephone the NASA STI Information Desk at 757-864-9658

- Write to:
  NASA STI Program
  Mail Stop 148
  NASA Langley Research Center
  Hampton, VA 23681-2199

NASA/TM—2018-219940

Low Power Radioisotope Conversion Technology and Performance Summary

Anthony J. Colozza
Vantage Partners, LLC, Brook Park, Ohio

Robert L. Cataldo
Glenn Research Center, Cleveland, Ohio

National Aeronautics and
Space Administration

Glenn Research Center
Cleveland, Ohio 44135

October 2018

Level of Review: This material has been technically reviewed by technical management.

Available from

NASA STI Program
Mail Stop 148
NASA Langley Research Center
Hampton, VA 23681-2199

National Technical Information Service
5285 Port Royal Road
Springfield, VA 22161
703-605-6000

This report is available in electronic form at http://www.sti.nasa.gov/ and http://ntrs.nasa.gov/

Low-Power Radioisotope Conversion Technology and Performance Summary

Anthony J. Colozza
Vantage Partners, LLC
Brook Park, Ohio 44142

Robert L. Cataldo
National Aeronautics and Space Administration
Glenn Research Center
Cleveland, Ohio 44135

Summary

This work presents a summary of low-power radioisotope-based power sources. This includes systems that use direct energy conversion from radioactive decay such as betavoltaics and systems that convert heat generated by the isotope decay. These types of power systems have terrestrial and space-based applications. Their main application is to provide low levels of power in remote environments where long life and reliability are the main objectives. This work looked at the potential performance of these types of systems and the range of output power they can achieve. Also considered was the amount of power that could be achieved from these different conversion technologies, while remaining under the critical limit acceptable for space flight without the need for special handling and controls. This is of interest for space missions where low power levels can be used for operating sensors or other devices, but the expense associated with the incorporation of radioactive material above this critical level would be cost prohibitive.

Nomenclature

ASRG	advanced Stirling radioisotope generator
CERN	European Organization for Nuclear Research
EB	electron beam
EBIC	electron beam induced current
FWPF	carbon-carbon composite woven with perpendicularly oriented graphite fiber
GPHS	general-purpose heat source
IR	infrared
MCNP	Monte Carlo N-Particle
MC–SET	Monte Carlo Simulation of Electron Trajectories
n-type	negative-type semiconductor
PIDEC	photon intermediate direct energy conversion
p-n	positive-negative
p-type	positive-type semiconductor
PG	pyrolytic graphite
PV	photovoltaic
RMD	Radiation Monitoring Devices, Inc.
RHU	radioisotope heater unit
SBIR	Small Business Innovation Research
TPV	thermophotovoltaic
UV	ultraviolet

Symbols

Av	Avogadro's number, 0.6×10^{24}
A_w	atomic weight of isotope
C	specific activity
c	speed of light, 2.998×10^{8}
E	energy per disintegration
E_p	energy of a photon
h	Planck's constant, 6.26×10^{-24}
I_{gen}	generated current
M	mass of plutonium
P	power density
P_{th}	thermal power
T_{cold}	heat out
T_{hot}	heat in
t	half-life in seconds
TBq	terabecquerel
t_{rad}	half-life of isotope in days
λ	decay constant

1.0 Low-Power Isotope Power Conversion Technologies

There are a number of different technologies and approaches for converting the heat generated or the radiation emitted from isotope radioactive decay into electrical power. These types of power sources can scale to small sizes and, therefore, have the potential for use in low-power, long-life applications, potentially providing a longer life alternative to batteries. There are a number of potential operational advantages to these types of power sources, which include the potential for high energy density, remote stand-alone operation and very long operational time. In addition, these technologies can use lower cost and more-abundant radioisotopes that are currently not considered viable for power production.

There has been interest in these devices for commercial, military, and space applications. These low-power, long-life sources are mainly being developed to replace batteries for remote and space applications. These types of devices are also applicable to harsh environments, such as high-temperature operation, where batteries may not be applicable. The U.S. military has recently shown considerable interest in the technology and is recommending a $25 million, 5-yr effort to further develop it (Ref. 1). Some potential applications for the low-power isotope systems include

- Sensors for remote applications (radiation sensor, etc.)
- Ultralow, long-life power device health monitoring
- Long-duration space missions where solar power is not an option
- On-chip nanopower source for compact self-contained electronics designs
- A trickle charge power source for battery charging

A number of these conversion technologies are currently at various levels of development from conceptual to near-flight-ready designs. These technologies are summarized in the following sections.

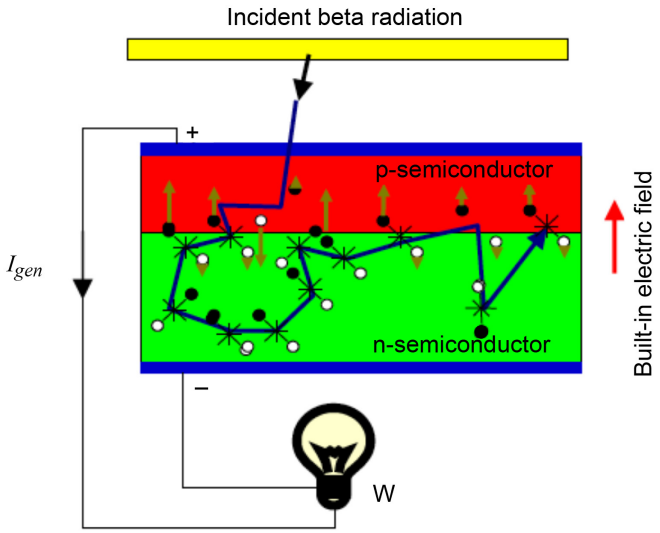

Figure 1.—Betavoltaic operational illustration, where I_{gen} is generated current.

1.1 Betavoltaics

A betavoltaic device directly converts beta particles (electrons) from a beta-emitting radioactive source into electrical energy. This is accomplished through a p-n junction conversion similar to that of a photovoltaic (PV) cell. The process of generating electricity with a betavoltaic cell is illustrated in Figure 1.

A betavoltaic cell generates electricity by the formation of electron-hole pairs within the semiconductor material through ionization from the beta particles emitted from the beta radiation source. An internal electric field produced within the semiconductor material separates the electrons and ions, causing the electrons to migrate to the n-semiconductor current collection plate. The electrons then flow through to the positive p-semiconductor current collection plate, completing the circuit and producing an electric current. The effective thickness of the beta source is limited due to self-absorption of the beta particles from within the radioactive material itself. For a given type of radioactive material, there is a maximum thickness beyond which the material will not produce any additional energy flux. These thicknesses are usually fairly thin, on the order of a few hundred nanometers, for example, for Ni^{63}, the thickness has been estimated to be approximately 2.2 μm (Ref. 2).

The main advantage of a betavoltaic system is the long operational lifetime of greater than 20 yr and a wide temperature operating range of approximately –50 to 150 °C. In addition to long life, other projected advantages include solid-state operation with no maintenance requirements and high-power density with direct nuclear-to-electric conversion.

The first commercial betavoltaic-based battery, shown in Figure 2, called a betacell was manufactured from 1968 to 1974. It used ^{147}Pm as the beta source. The output voltage of each cell was 0.5 V. The individual cells could be connected in series to increase the output voltage. A standard arrangement was 10 cells in series producing an output voltage of 5.0 V. The cells were constructed in 50-, 200-, and 400-μW units.

Another commercially available betavoltaic device called NanoTritium™ is manufactured by City Labs, Inc. This power source is for providing low-level power to electronics boards. It is manufactured in an electronic chip form as shown in Figure 3.

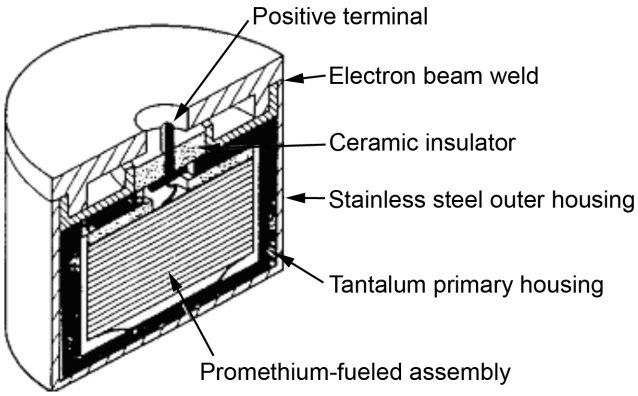

Figure 2.—Commercial ^{147}Pm-based betavoltaic power source.

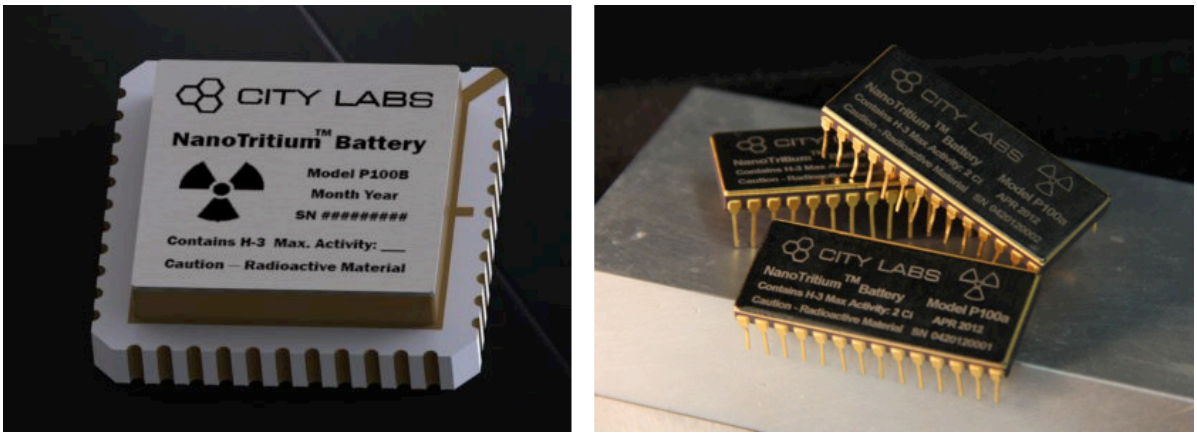

Figure 3.—NanoTritium™ betavoltaic power source. Copyright City Labs, Inc.; used with permission.

The NanoTritium™ source uses T as the radioactive isotope for generating the beta particles. It can produce an output voltage of 0.8 to 1.1 V with a current density of 150 nA/cm^2. To make the T source, T gas is loaded into a hydride material, such as Mg, Ti, or Sc, and subjected to high pressure and temperature. Experimentation has shown that the hydride material will hold the T gas for extended periods of time with little to no loss. For example, a loaded TiH_2 will lose only 8 percent of the gas over a 12.3-yr period.

There are a number of drawbacks to the betavoltaic energy conversion device. These are mainly due to the beta radiation exposure, which can damage the p- and n-junction semiconductor material. This damage also limits the lifetime of the device. Historically, the efficiency of these devices has been low, on the order of a few percent. To reduce the potential for radiation damage, isotopes with emissions energies below 300 keV can be selected. However, using lower emission energies will reduce the output power density of the system.

To provide greater flexibility and operational capability, combined hybrid battery and betavoltaic devices are being developed. These devices utilize a battery in conjunction with a betavoltaic power source. The betavoltaic source is used for low power output (0.1 to 10 μW) and to trickle charge the battery. The battery is used to provide high power output (30 to 100 mW) for short periods of time. This burst power capability can significantly increase the applications where a betavoltaic power source can be used.

Additional development is also being done on modeling the temperature effects on the power production from the betavoltaic device. This is being done through computer modeling with programs such as MATLAB® and Simulink® (MathWorks®). Another area of development is in the material properties of the semiconductor material used to convert the beta particle energy to electrical power.

These materials can be analyzed by using an electron beam induced current (EBIC) to identify critical properties and parameters of the semiconductor material such as the diffusion length, surface defect density, and doping concentrations. This type of experimentation can also be used to observe the effects of magnetic and electrostatic fields. Some of this experimental work is being carried out by the Naval Surface Warfare Center at Crane, Indiana. Simulation work is also being performed to explore the interaction of beta particles with surrounding material. These simulations are being performed at research institutes such as the European Organization for Nuclear Research (CERN) by using their Geant4 simulation platform, which simulates the passage of particles through matter, or at Oak Ridge and Los Alamos national laboratories by using their general-purpose Monte Carlo N-Particle (MCNP) simulation for modeling neutron, electron, and photon transport. In addition, other simulation tools can also be utilized, such as Monte Carlo Simulation of Electron Trajectories (MC–SET), to simulate electron trajectories in a material by using a Monte Carlo analysis.

Ultimately, the amount of power that can be extracted from the decay of an isotope is based on the emission energy and rate of the isotope. From these characteristics, the power density (P, in W/gm) can be calculated by Equation (1) (Ref. 3), where the specific activity (C) of an isotope or Ci/g is given by Equation (2), t_{rad} is the half-life of the isotope in days, and A_w is its atomic weight (Ref. 4). The energy per disintegration (E) is given in MeV. The conversion factors of 3.7×10^{10} dis/s/ci and 1.603×10^{-13} W/MeV/s are combined to give the constant (5.931×10^{-3}) used in Equation (1).

$$P = (5.931\times10^{-3})CE \tag{1}$$

$$C = \frac{1.3\times10^{8}}{t_{rad}A_w} \tag{2}$$

A number of different isotopes can be utilized as beta emitters. Some potential beta-emitting isotopes are listed in Table I.

A majority of the betavoltaic work currently being conducted is performed at universities or in government laboratories. However, there are a few commercial companies (City Labs, Inc. and Widetronix Inc.) that are developing commercially available betavoltaic products. Some of this recent or ongoing work is summarized in this section.

The University of Missouri is working on a generation 2 device. This device utilizes a layer of radioactive material embedded in the semiconductor layer. Si is not utilized in the device. The device is compact and provides self-shielding. For their design, ^{35}S is the beta-emitting material and Se is the electrical conversion material.

The pure beta emitter, ^{35}S, has energies between 49 and 167 keV and a half-life of 87.3 d. The emitted beta radiation has an interactive range of approximately 26 cm in air and can be shielded with 200 μm of plastic. It has a low melting temperature of 115 °C and is fairly easy to work with.

Se is easy to fabricate with a low melting temperature of 221 °C. It is a positive-type (p-type) semiconductor in both its solid and liquid states with an energy band gap of 1.8 to 2.0 eV. It is chemically compatible with the selected radioactive source material, S.

The performance of the generation 1 and 2 devices is summarized in Table II. For the generation 1 device, the current decreased steadily from the short circuit value of 107.4 to 0 nA at the open circuit voltage of 0.9 V. For generation 2, the short circuit current was much higher at 752 nA and decreased linearly to approximately 80 nA at 0.4 V. From there, it gradually decreased to 0 nA at the open circuit voltage of 1.0 V. For generation 1 the maximum power output occurred at approximately 0.4 V and for generation 2 it occurred at approximately 0.2 V.

TABLE I.—BETA-EMITTING ISOTOPES (REFS. 5 TO 8)

Isotope	Daughter products	Average decay energy, MeV	Half-life, yr	Power density, W/g
^{3}H (Tritium)	^{3}He	0.00569 (β)	12.3	0.325
^{22}Na	^{22}Ne	0.2155 (β) 0.5112 (γ)	2.6	7.99
^{35}S	^{35}Cl	0.16718 (β)	0.24	42.34
^{42}Ar	^{42}K, ^{42}Ca	0.598 MeV (β)	32.9	0.922
^{60}Co	^{60}Ni	0.08579 (β) 1,332.5 (γ) 1,173.2 (γ)	5.27	0.577
^{63}Ni	^{63}Cu	0.01743 (β)	100.1	0.0059
^{85}Kr	^{85}Rb	0.251 (β) 0.514 (γ)	10.8	0.582
^{90}Sr	^{90}Y, ^{90}Zr	0.196 (β)	28.8	0.161
^{106}Ru	^{106}Rh, ^{106}Pd	0.01003 (β)	1.02	0.196
^{113}Cd	^{113}In	0.019 (β)	14.1	0.025
^{125}Sb	^{125}Te	0.087(β) 0.427 (γ)	2.76	0.536
^{129}I	^{129}Xe	0.15 (β)	1.57×10^{7}	1.574×10^{-7}
^{137}Cs	^{137}Ba	0.1568 (β) 0.66164 (γ)	30.1	0.081
^{147}Pm	^{147}Sm, ^{143}Nd	0.06196 (β)	2.6	0.341
^{151}Sm	^{151}Eu	0.01968 (β)	88.8	0.003
^{155}Eu	^{155}Gd	0.0374 (β) 0.105 (γ) 0.087 (γ)	4.67	0.108
^{171}Tm	^{171}Yb	0.0251 (β)	1.92	0.162
^{194}Os	^{194}Ir, ^{194}Pt	0.097 (β)	6.0	0.176
^{204}Tl	^{204}Pb, ^{204}Hg	0.345 (β)	3.78	0.952
^{210}Pb	^{206}Pb	0.017 (β) 0.047 (γ)	22.3	0.0077
^{227}Ac	^{207}Pb, ^{205}Ti	0.0111 (β) 5.042 (α)	21.8	0.0048
^{228}Th	^{224}Ra	0.108 (α)	1.91	0.526
^{232}U	^{228}Th	5.20 (α)	69.8	0.692
^{238}Pu	^{234}U	5.4991 (α)	87.84	0.558
^{241}Pu	^{241}Am	0.00523 (β)	14.4	0.0032
^{243}Cm	^{239}Pu	6.1688 (α)	29.1	1.851

TABLE II.—BETAVOLTAIC CELL PERFORMANCE OF ^{35}S AND Se

Value	Generation 1	Generation 2
Radioactivity, mCi	10.89	33.61
Max. output power, nW	76.53	687.0
Open circuit voltage, V	0.899	0.864
Short circuit current, nA	107.4	752.0
Efficiency, percent	2.42	7.05
Cell dimensions, cm	3.81 long by 2.54 wide by 0.2 high (1.93 cm^3 volume)	3.81 long by 2.54 wide by 0.2 high (1.93 cm^3 volume)

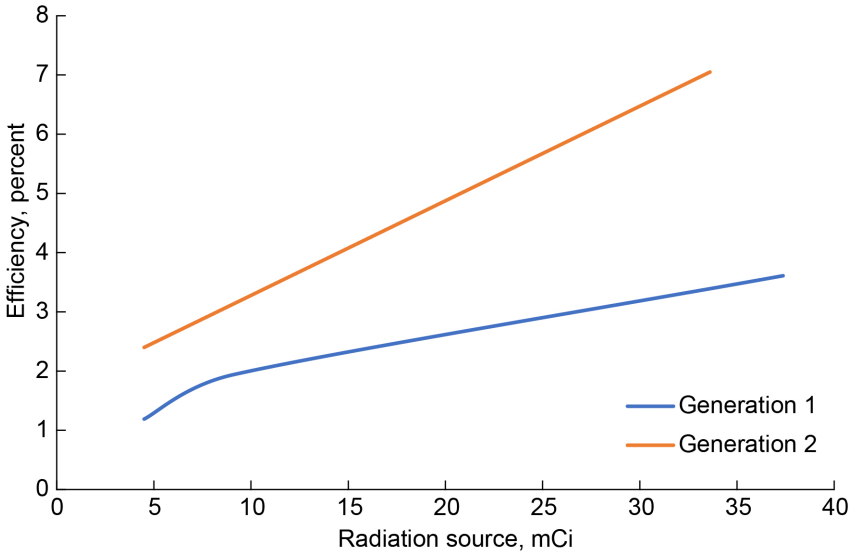

Figure 4.—Efficiency versus radiation source intensity.

Based on the results given for the University of Missouri-developed betavoltaic converter, the overall efficiency is dependent on the source radiation dose. For both the generation 1 and 2 devices, the change in efficiency as a function of the radiation source intensity is given in Figure 4.

The University of Illinois is looking into a p-n junction betavoltaic device for producing long-life low power by using radioisotopes from nuclear waste. Their proposed system utilizes ^{63}Ni as the beta source and Si as the semiconductor material for the p-n junction. This combination of semiconductor and beta source was selected because the energy level of the beta particles released by the ^{63}Ni is below the damage threshold of Si of 200 to 250 keV. Modifications to the design are being considered to utilize higher energy emitters such as ^{90}Sr, which can be obtained from nuclear waste. The device being developed is a planar geometry where the p-n junctions are etched into a Si wafer similar to the process of solar cell construction. Each cell on the wafer is 12 by 17 mm (Ref. 9). The ^{63}Ni is electrodeposited on each cell over an area of approximately 1 cm^2. Initial test results from a prototype wafer produced 2.5 pW of power at 0.4 mV with a conversion efficiency of 0.0005 percent. To improve on the performance, a porous design is being considered to increase the number of beta particles that can interact with the p-n junction and, therefore, increase overall efficiency. This geometry change is illustrated in Figure 5.

Another approach to capture and convert a greater fraction of the generated beta particles is to utilize multiple p-n junctions inline with the emitter. A prototype multiple-junction device was constructed with a stack of five p-n junctions. This device produced a maximum output power of 1.15 nW with a conversion efficiency of 3.57 percent.

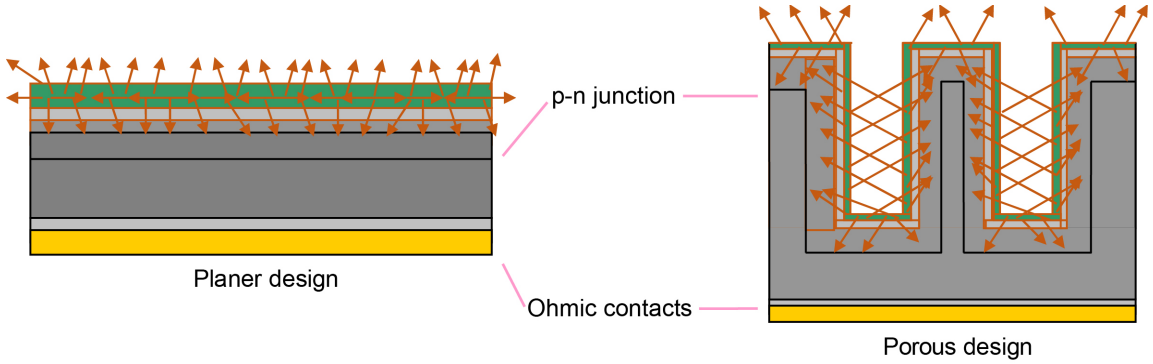

Figure 5.—Proposed geometry improvement to enhance beta interaction (Ref. 9).

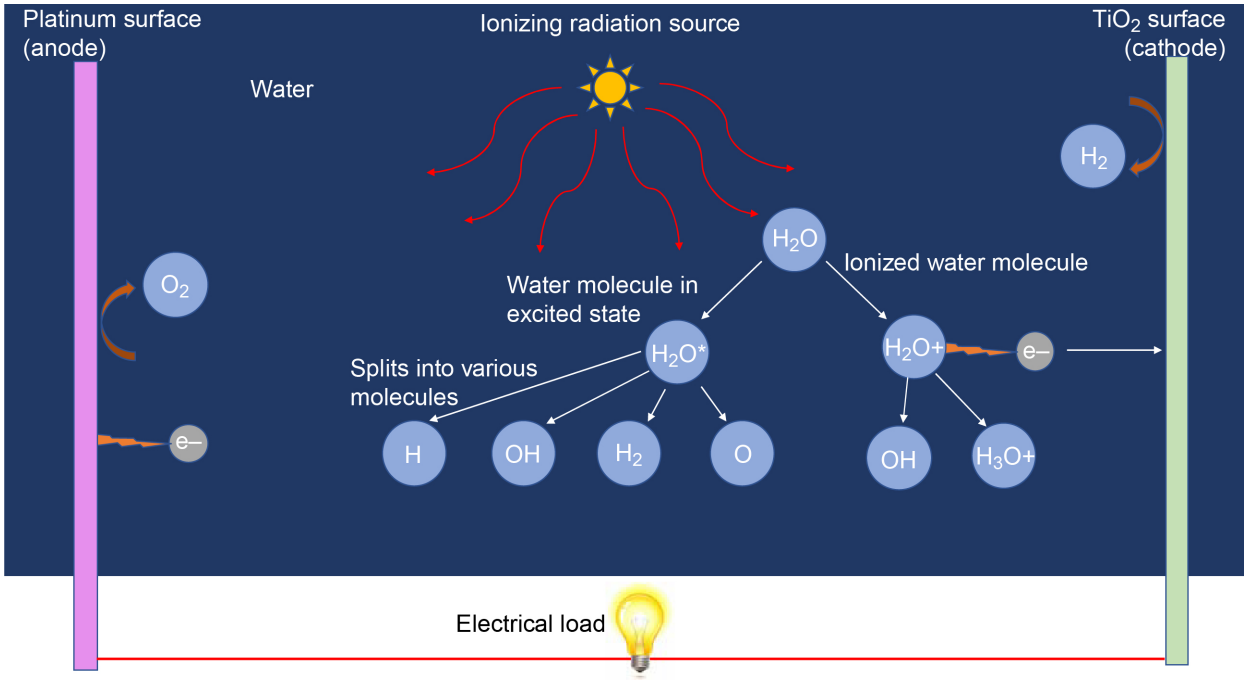

Figure 6.—Betavoltaic water radiolysis process.

1.2 Water Radiolysis Betavoltaics

A variation on the betavoltaic system described previously is a betavoltaic converter that utilizes a water-based solution with the process of radiolysis, or the dissociation of molecules through exposure to ionizing radiation, and surface plasmons (Ref. 10). A surface plasmon is an interface between two materials, a conductor and a nonconductor, where electron oscillations take place. The presence of radiation causes an electromagnetic field to form at this interface, which in turn causes the electron density to vary across the boundary of the materials. This process is illustrated in Figure 6 for a TiO_2 and Pt electrodes.

Water exposed to a beta emitter will break down through the radiolysis process into a number of different molecules such as H^-, HO^-, HO_2^-, OH^-, H_3O+, H_2, and H_2O_2. Most of the energy transferred to the water through radioactive decay goes into creating these molecules and free electrons. Some of the energy, however, goes into producing surface plasmons in conjunction with a Pt surface. The Pt surface

acts as an anode and a TiO_2 surface as the cathode. The internal field between these electrodes causes the electrons to migrate to the TiO_2 surface producing an electric current.

The University of Missouri is also looking at a betavoltaic device based on the water radiolysis process. For this process, ^{90}Sr is used. The isotope, ^{90}Sr, has a half-life of 28.68 yr and decays through beta emissions of 0.546 MeV maximum, 0.1958 MeV average to ^{90}Y with a half-life of 2.67 days. The ^{90}Y in turn decays to the stable isotope ^{90}Zr through beta emissions of 2.28 MeV maximum (0.9337 MeV average).

A test cell using this concept produced 75.02 $\mu W/cm^2$ with a conversion efficiency of 53.88 percent of the power inputted from the radiation source.

1.3 Photon Intermediate Direct Energy Conversion (PIDEC)

Another similar process of direct conversion of radiation from nuclear decay to electrical power is termed PIDEC (Ref. 11). This is similar to the betavoltaic process except that it uses any type of radiation (neutrons, gamma, beta, or alpha) released through radioactive decay or from a nuclear reaction to cause a gas or material to fluoresce-emitting photons that are in turn converted into electricity through a PV converter that is tuned to their frequency. The fluoresce process is termed excimer fluorescence. A diagram illustrating this process is shown in Figure 7.

This process has a number of characteristics that are beneficial to the energy conversion process. Radiation damage to the converter cell is minimized because it is shielded from the radiation source. The process has the potential for high-efficiency conversion, in the range 10 to 40 percent. Another benefit is that this conversion process is not restricted to a particular radiation type. Alpha and beta particles, x-rays and gamma radiation and neutrons can all be used to produce the reaction. The state of the radioisotope radiation source is not fixed; it can be a solid, liquid, or gas. The frequency band of the excimer photon emission process is relatively narrow. This makes conversion easier than over a wide band and a cell tuned to this frequency can provide high conversion efficiencies.

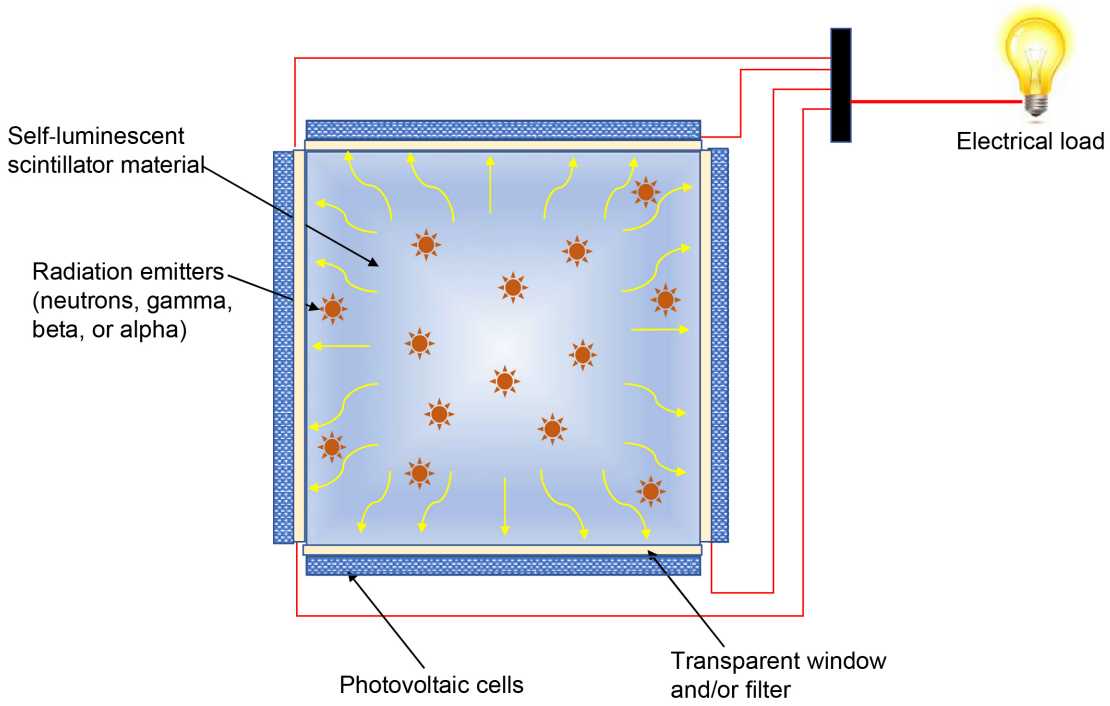

Figure 7.—Photon intermediate direct energy conversion electrical power generation process.

There are a number of potential excimer fluorescence materials. These materials vary in their efficiency to generate photons or fluoresce when exposed to the radioactive source. A list of material types, fluorescence wavelength and the fluorescence efficiency is given in Table III. Some data on the fluorescence efficiency was not available for some of the excimer materials listed in the table.

TABLE III.—EXCIMER MATERIALS AND FLUORESCENCE EFFICIENCIES (REFS. 12 TO 19)

Excimer material	Emission wavelength (nm, peak)	Fluorescence efficiency (quantum yield)	Matched PV[a] cell material	Max. PV cell efficiency	Max. total conversion efficiency
NeF	108	0.43	AlN	0.477	0.21
Ar_2	129	0.50	AlN	0.645	0.32
Kr_2	147	0.47	AlN, diamond	0.789 0.655	0.35 0.31
F_2	158	0.44	AlN, diamond	0.821 0.703	0.36 0.31
Xe_2	172	0.48	AlN, diamond	0.861 0.764	0.41 0.37
ArCl	175	0.48	AlN, diamond	0.876 0.776	0.42 0.37
KrI	185	0.37	AlN, diamond	0.928 0.823	0.34 0.31
ArF	193	0.35	AlN, diamond	0.969 0.859	0.34 0.30
KrBr	206	0.33	Diamond, SiC	0.917	0.30
KrCl	222	0.31	Diamond, SiC	0.982	0.30
$LaPO_4$-PR	225 to 265	0.35	Diamond, SiC	0.71	0.25
KrF	249	0.28	SiC	0.64	0.18
XeI	253	0.37	SiC	0.645	0.24
Cl_2	258	0.32	SiC	0.68	0.22
XeBr	282	0.29	SiC	0.7	0.20
Br_2	290	0.29	SiC	0.61	0.18
XeCl	308	0.27	SiC	0.48	0.13
I_2	343	0.24	SiC	0.25	0.06
$LiGdCl_4$	345, 365	-----	InGaN, SiC	0.51	-----
XeF	346	0.24	InGaN, SiC	0.30	0.07
$CeCl_3$	350	-----	InGaN, SiC	0.35	-----
$LaBr_3$	356, 387	-----	InGaN, SiC	0.68	-----
Cs_2LiYCl_6	370	-----	InGaN, SiC	0.54	-----
$CeBr_3$	371	-----	InGaN, SiC	0.55	-----
$Gd_2Si_2O_7$	372, 394	-----	InGaN, SiC	0.705	-----
K_2LaI_5	401, 439	-----	InGaN, SiC	0.67	-----
Kr_2F	415	0.17	InGaP, SiC	0.76	0.13
NaI	415	0.61	InGaP, SiC	0.76	0.46
BaI_2	425	-----	InGaP, SiC	0.79	-----

TABLE III.—EXCIMER MATERIALS AND FLUORESCENCE EFFICIENCIES (REFS. 12 TO 19)

Excimer material	Emission wavelength (nm, peak)	Fluorescence efficiency (quantum yield)	Matched PV[a] cell material	Max. PV cell efficiency	Max. total conversion efficiency
CsI	425	0.70	InGaP, SiC	0.79	0.55
Ba_2CsI_5	435	-----	InGaP, SiC	0.81	-----
Cs_2BaI_5	435	-----	InGaP, SiC	0.81	-----
SrI_2	435	0.20	InGaP, SiC	0.81	0.16
Na_2	437	0.46	InGaP, SiC	0.81	0.37
HgI	443	0.19	InGaP, SiC	0.82	0.16
ZnS	450	-----	InGaP, SiC	0.83	-----
Li_2	459	0.42	InGaP, SiC	0.84	0.35
CaI_2	470	-----	InGaP, SiC	0.85	-----
Hg_2	480	0.21	InGaP, SiC	0.86	0.18
$SrZrO_3$	480	-----	InGaP, SiC	0.86	-----
$SrHfO_3$	480	-----	InGaP, SiC	0.86	-----
HgBr	502	0.17	InGaP	0.87	0.15
LuI_3	522	-----	InGaP	0.84	-----
CsI	530	0.20	InGaP	0.82	0.16
KrO	547	0.15	InGaP	0.81	0.12
XeO	547	0.15	InGaP	0.81	0.12
YI_3	549	-----	InGaP	0.80	-----
HgCl	558	0.15	InGaP	0.78	0.12
K_2	575	0.42	InGaP	0.77	0.32
GLuGAG (ceramic)	580	-----	InGaP	0.76	-----
Rb_2	605	0.41	InGaP	0.75	0.31
ZnSe	640	-----	InGaP	0.65	-----
CdI	655	0.13	InGaP	0.62	0.08
Cs_2	713	0.37	GaAs	0.88	0.33
CdBr	811	0.10	GaAs	0.87	0.09

[a]Photovoltaic.

It should be noted that self-absorption of the fluorescence spectrum can significantly reduce the overall efficiency of a fluorescence-based system. Ideally, the fluorescence material would have no overlap between the fluorescence and absorption spectrums. The difference between peaks of the absorption and emission spectrum of the material, given in nm, is represented by the Stokes shift for that material as illustrated in Figure 8. Materials that have larger Stokes shifts will be more applicable to a PIDEC system and produce higher overall efficiencies.

Also shown in Table III are potential PV cell materials whose conversion band gap is matched to the emission fluorescence spectrum of the excimer material. One of the potential PV materials listed is diamond. Diamond is an intriguing PV cell material since it is much less susceptible to radiation damage than other conversion materials such as SiC, GaN, or AlN. It has also been successfully utilized as a radiation detection material for neutrons and gamma and beta radiation at high fluxes. It can also operate

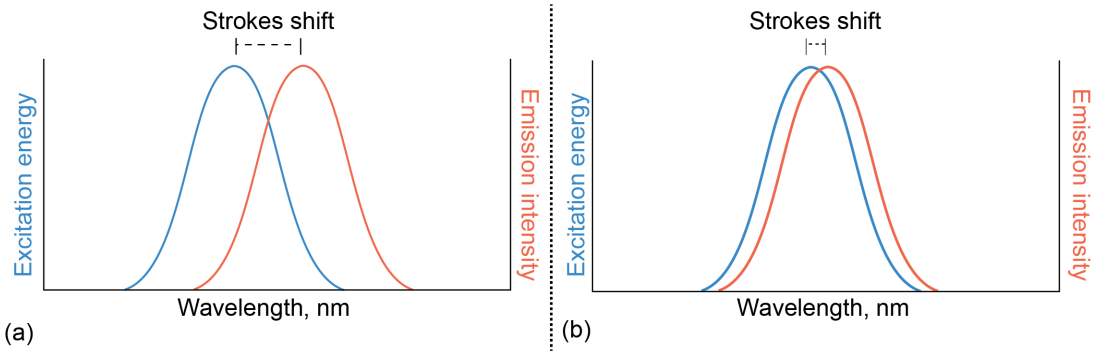

Figure 8.—Stokes shift of a material (Ref. 20).

TABLE IV.—BAND GAP AND ABSORPTION WAVELENGTH FOR POTENTIAL ULTRAVIOLET PHOTOVOLTAIC MATERIALS (REFS. 23 TO 26)

Material	Band gap, eV	Wavelength, nm
AlN	6.2	200.0
3C-SiC	6.0	206.6
Diamond	5.5	225.4
4H-SiC	3.23	383.8
6H-SiC	2.86	433.5

at high temperatures, has a very high thermal conductivity of 2,600 W/mK, which is about 6.5 times greater than copper, and is an excellent electrical insulator. The production of large-area, single-crystal diamond layers is not currently commercially available. However, there has been significant progress in this area by using hot filament chemical vapor deposition and ion bombardment induced buried lateral growth (Refs. 21 and 22).

There is limited data on the efficiency versus spectrum for some of the new PV cell material that can potentially operate within the ultraviolet (UV) spectrum. However, their theoretical band gap can be used to estimate the photon wavelength that would be effective with the given PV cell material. The band gap energy of a material is the gap in energy between the bound state of an electron and its free state. Therefore, the energy required to break free an electron from its bound state within an atom of a given material is the band gap energy. A photon of this energy will excite an electron into a free state, which enables the electron to move freely within the material producing the electric current from the PV cell. The energy of a photon (E_p) is given by Equation (3), which is based on Planck's constant (h, 6.626×10^{-24} J/s) and the speed of light (c, 2.998×10^{8} m/s).

$$E_p = \frac{h\,c}{\lambda} \tag{3}$$

The band gap for some potential UV conversion PV materials is given in Table IV.

Another radiation energy conversion concept being evaluated at the University of Missouri is based on the PIDEC process. The process utilizes ^{85}Kr as the radiation emitter as well as the excimer material (Kr_2) that fluoresces. The proposed design utilized a pressurized sphere with ^{85}Kr gas at 676 atm. The

interior of the sphere is covered with UV-tuned PV cells to convert the florescence from the ^{85}Kr to electrical power. The estimated output of the system is 8 W/kg.

The krypton isotope, ^{85}Kr, is relatively rare. However, it is a byproduct of fission in conventional nuclear power plants. Collecting this gas from fission reactors would provide an adequate supply for use in PIDEC devices. In addition, the emission wavelength of ^{85}Kr can be shifted by mixing it with halide gases, such as Fl, Br, or Cl, producing KrF, KrBr, or KrCl.

This process uses the absorption of beta radiation to cause a material to fluoresce similar to the layout illustrated in Figure 7, except that the radiation source is solely beta emitters. The light given off through the fluorescence process is converted to electrical power through a tuned PV cell. The beta emissions produced are completely absorbed in the photon-emitting material. This enables an efficient use of the radioactive material and produces a monochromatic light output through fluorescence of the material, which can be matched to a PV cell for high-energy conversion efficiency.

In another process being developed, $^{90}SrI_2$, can be used as both the beta emitter and the fluorescence material. The estimated efficiency of conversion for SrI_2 fluorescence, as given in Table III is 16 percent. The estimated electrical specific output power is 0.22 W/kg.

Photodiodes were tested to convert the fluorescence emitted by the ^{90}Sr source by using Si PIN diodes (Hamamatsu Photonics). For a 1- by 1-in. crystal, an output power of 6.37 nW was achieved with a 0.894-mCi source. Radiation Monitoring Devices Inc. (RMD) has successfully demonstrated a beta-source power generation device by using SrI_2 as both beta-emitting material (^{90}Sr) and fluorescence material (SrI_2). The material showed that 0.1-percent seeding or greater of SrI_2 with ^{90}Sr is possible without excessive radiation damage. A CsI:Tl system was also constructed. This material has 1-percent ^{204}Tl in the CsI fluorescence emitter.

The U.S. Army Research Laboratory is constructing an experimental power source termed iBAT that can produce over 100 μW of electrical power. The isotope battery utilizes a series of cells or packets to achieve the desired output power level. Each cell is constructed of a sandwich of ^{63}Ni phosphor mix between two outer layers of PV cells. Each of these cells produces approximately 2.3 μW of electrical power. Six of these cells are wired together into a packet and up to 10 packets are interconnected to produce the isotope battery. An example is shown in Figure 9.

Figure 9.—U.S. Army Research Laboratory isotope battery prototype.

The U.S. Army Research Laboratory has also recently funded a number of Small Business Innovation Research (SBIR) projects with the goal of developing betavoltaic-type devices for producing a long-life power source for unattended sensors or network communication nodes. Some examples include an SBIR phase I program conducted by Widetronix (W911QX-15-C-0047), which is developing a projected 12-percent efficient SiC direct energy conversion device. Another phase I SBIR was with Infinity (W911QX-15-C-0046) and utilized a higher risk, more novel electrochemistry approach with projected efficiencies in the 70-percent range. A third phase I SBIR with Physical Sciences (W911QX-15-C-0043) was to produce high-volume, low-cost, thin-film PV manufacturing capability for cells tuned to frequencies compatible with isotope beta emissions. The goal is for greater than 10-percent conversion efficiency with beta emissions of 5 keV.

1.4 Alphavoltaics

Alphavoltaics is a similar process to the betavoltaics described in Section 1.1, except that it utilizes alpha radiation (an ionized He atom consisting of two protons and two neutrons) instead of beta radiation. Alpha emitters are commonly used in commercial items such as smoke detectors. Alpha radiation is easily shielded with the common claim that alpha particles can be stopped with a sheet of paper. The main drawback to alpha radiation is the damage it can do when it does interact with matter. Therefore, any alphavoltaic device needs to be constructed by using materials that are radiation tolerant.

1.5 Isotope Heat Conversion

1.5.1 Thermoelectric Converter

Low-power thermoelectric converts utilize a radioisotope heater unit (RHU) as the heat source and solid-state electric power converters that operate based on the Seebeck effect by using a thermoelectric converter. In some designs, a rechargeable Li-ion battery is also used to provide higher output power levels for short durations. The battery is then recharged by the RHU power source. Thermoelectric converters operate by generating a temperature difference across the p-type and negative-type (n-type) semiconductor materials (Ref. 27). In the n-type material, the charge carriers are negatively charged electrons, whereas in the p-type material, they are positively charged ions. When a temperature gradient is placed across the material, a charge builds up on the cold side of the material (electrons and ions). An electric field is generated due to the charge buildup and this produces a voltage difference between the hot and cold sides. This voltage difference will drive current between the p- and n-type material if they are connected in a circuit. This arrangement is illustrated in Figure 10.

The RHU is a lightweight standard heat source designed to provide 1.1 W of thermal power at the beginning of life. It consists of a cylinder 32 mm high by 26 mm in diameter, weighing approximately 40 g. Within the cylinder is the pelletized ^{238}Pu radioscope material encapsulated within a Pt alloy shell and surrounded by graphite thermal insulation. This layout is shown in Figure 11.

The decay of ^{238}Pu generates alpha particles whose energy is quickly converted into heat as they interact with nearby material. This makes the ^{238}Pu isotope an ideal heat source. A thermoelectric converter, or thermopile, is then used to convert this heat into electrical power. This arrangement is illustrated in Figure 12.

A current thermoelectric design from Hi-Z Technology, Inc., to be utilized with an RHU uses p- and n-doped Bi_2Te_3 (Refs. 29 and 30). Other manufacturers of similar types of thermoelectric converters included The Institute of Thermoelectricity in Chernivtsi, Ukraine, and Swales Aerospace. These devices were capable of producing 40 mW of power with a hot side temperature of approximately 200 °C and a cold side temperature of approximately 30 °C (Ref. 30). The mass of the thermoelectric power conversion

module is approximately 7 g. Combined with the RHU, the total power converter mass is approximately 47 g with a specific mass of 0.85 W/kg. The thermal to electrical conversion efficiency is approximately 4 percent.

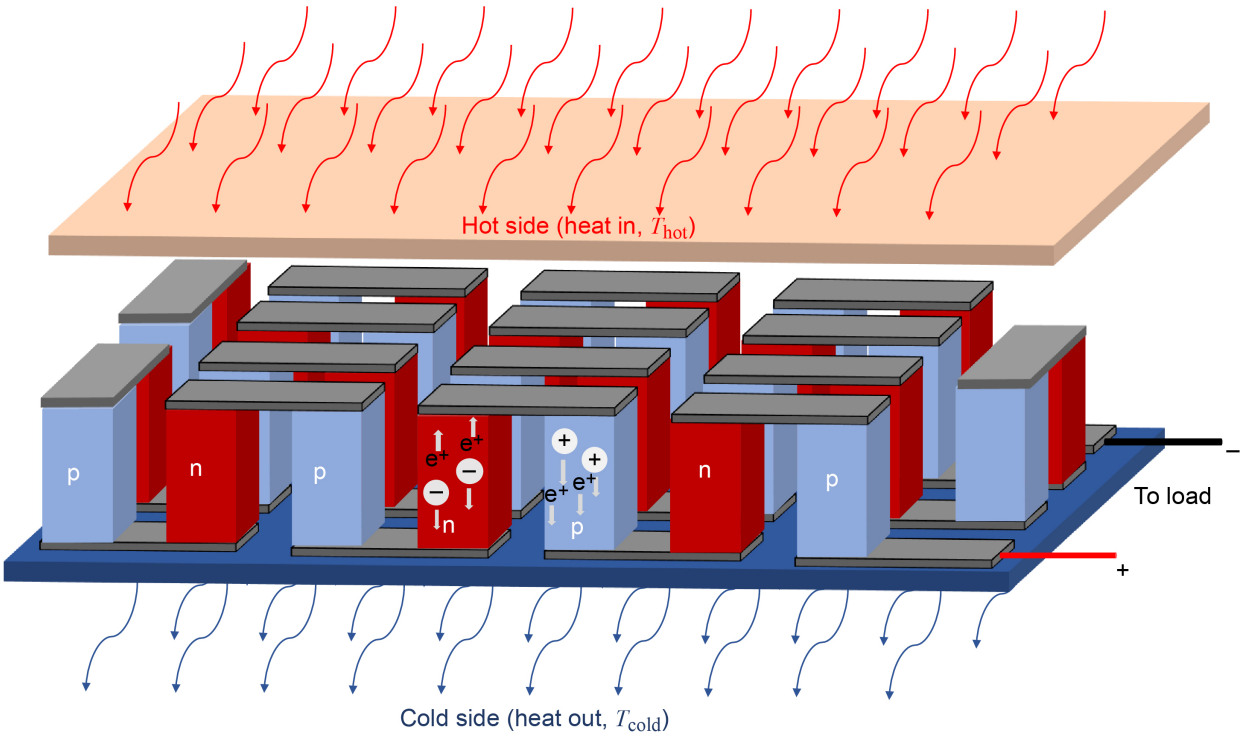

Figure 10.—Thermoelectric power generation illustration.

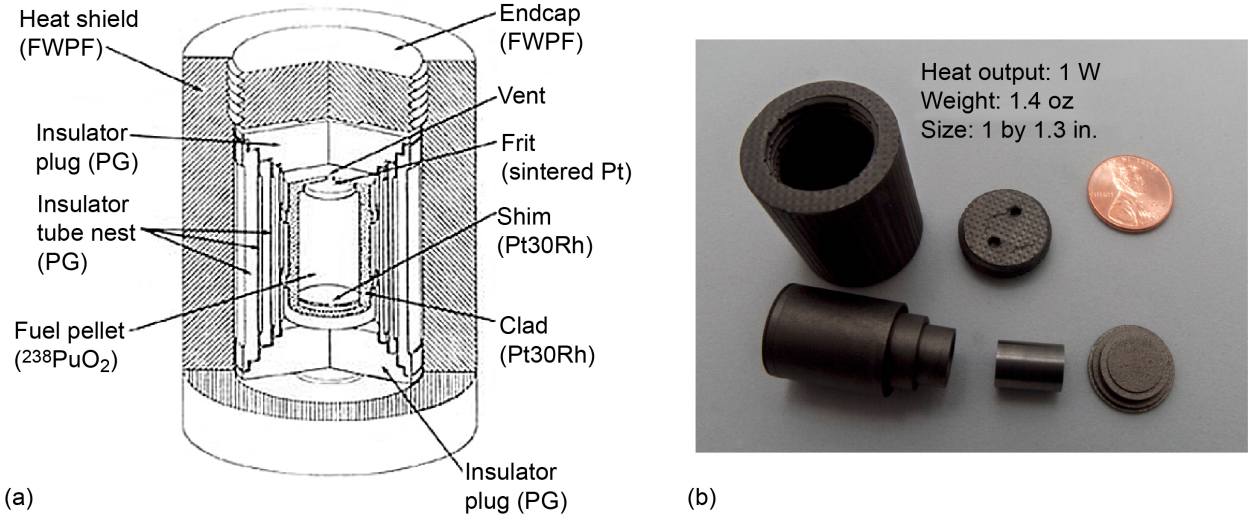

Figure 11.—Radioisotope heater unit components (Ref. 28). (a) Radioisotope heater cutaway view. FWPF is a carbon-carbon composite woven with perpendicularly oriented graphite fiber and PG is pyrolytic graphite. (b) Radioisotope heater unit and components and size comparison. Heat output of 1 W, weight of 1.4 oz., dimensions of 1 by 1.3 in.

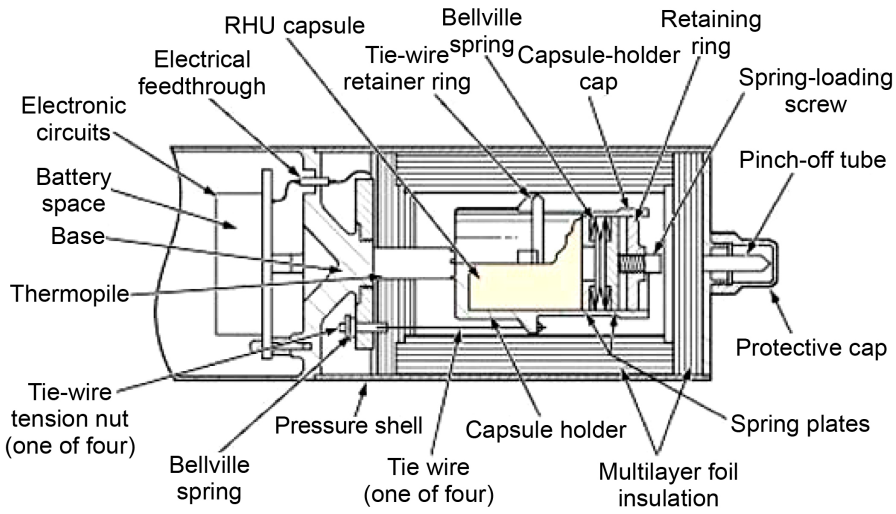

Figure 12.—Radioisotope heater unit (RHU) thermoelectric power source (Ref. 29).

The mass of ^{238}Pu needed (M) to generate the 1 W of thermal power (P_{th}) produced by an RHU can be calculated from Equation (4).

$$M = \frac{P_{th} MW}{E \lambda \mathrm{A_v}} \tag{4}$$

Where $\mathrm{A_v}$ is Avogadro's number (0.6×10^{24} [nuclei/mol]), E is the energy per disintegration for ^{238}Pu (5.4991 MeV, from Table I) and the decay constant (λ) is given by Equation (5) for the half-life (t) given in seconds.

$$\lambda = \frac{\ln(2)}{t} \tag{5}$$

To convert the energy per disintegration from MeV to W, it needs to be multiplied by 1.6×10^{-13} W/(MeV/s) similarly to Equation (1). From the previous equations, 1 W of thermal power will require 1.8 g of ^{238}Pu.

1.5.2 Thermionics

Similar to thermoelectrics, thermionics produce power through heat produced by the radioisotope. However, their means of power production is very different. Whereas the thermoelectric power is generated based on charge buildup due to a temperature difference across a material, thermionics produce power by the thermionic emission of electrons from a hot surface. This process is illustrated in Figure 13.

For thermionics to work the hot surface needs to have a low work function, on the order of 3 eV. Electrons produced are collected at a lower work function collector, on the order of 1.5 eV or less. The emitter and collector are separated by a small gap, on the order of 0.2 mm. For efficient operation, the gap needs to be less than the mean free path of the electrons to prevent them from returning to the emitter before impacting the collector. This however is difficult to achieve. Therefore, other means of preventing electron return to the cathode were devised. The main approach utilizes a gas such as Cs to fill the space between the cathode and anode. This gas nullifies the space charge effect, which causes the electrons to return to the cathode. Typical thermal to electrical conversion efficiencies of thermionic converters are within the range of 5 to 20 percent, depending on the operating conditions. Theoretical efficiencies are greater than 50 percent (Ref. 31).

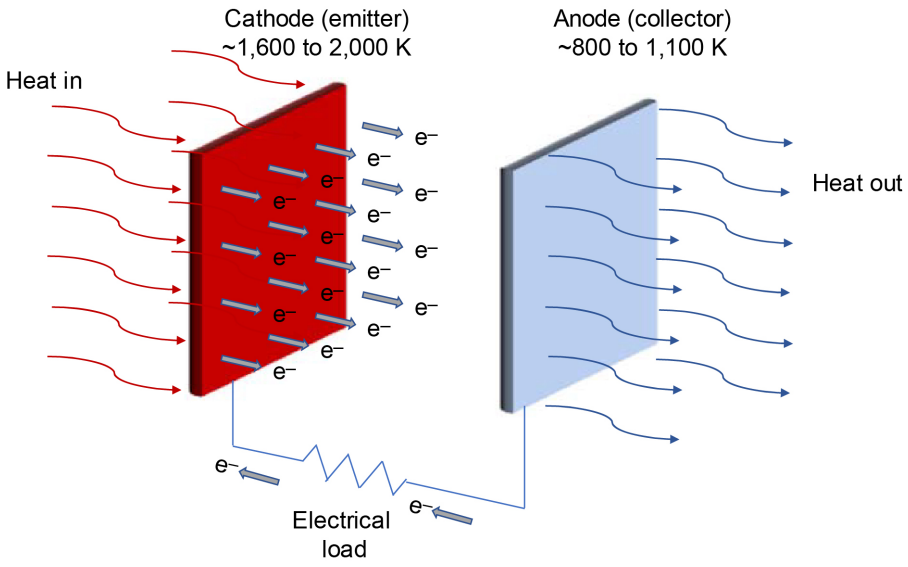

Figure 13.—Thermionic operation.

The advantages of a thermionic conversion system are long operating lifetimes and a high specific power due to their lightweight construction. The conversion efficiency of a thermionic converter tends to be higher than that of a thermoelectric converter. This is due to the higher operating temperature and corresponding temperature difference between the hot and cold side of the converter. This higher temperature difference corresponds to a higher Carnot efficiency. Also, in a thermoelectric converter, the heat losses between the hot and cold side are due mainly to conduction through the p-n junctions. Whereas for the thermoelectric system they are due solely to radiation since there is no contact between the hot and cold sides. For the temperature ranges commonly used, the heat losses through radiation in a thermionic system tend to be less than those from conduction in a thermoelectric system.

The main issue with a thermionic system is the required high operating temperature for the hot side of the converter. Generating this temperature, especially with a small amount of radioisotope material, is difficult and requires a well-insulated and sealed system to minimize any heat loss to the surroundings. Sufficiently limiting the heat losses to the surroundings to achieve the desired high temperatures and efficiency may not be possible under certain configurations.

1.5.3 Thermophotovoltaics (TPVs)

A TPV power source is similar to the betavoltaic power source in which PV cells are used to generate power from a photon source. In the case of betavoltaics, that source is the fluorescence of a material caused by the absorption of beta particles. For TPVs, the PV cell directly converts the infrared (IR) radiation emitted from a warm or hot body. This contrasts with a common PV cell, which is efficient at converting portions of the visible light spectrum to electricity. The IR portion of the spectrum has a larger wavelength and lower frequency than that of the visible portion. Therefore, the type of PV cell that can efficiently convert the IR portion of the spectrum is different than those used for visible light.

For a typical heat source emitting as a blackbody, the output spectrum will depend on its temperature as illustrated in Figure 14. As the temperature increases, the peak output frequency increases (wavelength decreases) toward the visible portion of the spectrum. Also, it should be noted that as the temperature increases, the total available energy, given by the area under the curves in Figure 14, also increases. Therefore, the higher the temperature of the emitting source, the greater the potential energy that can be collected.

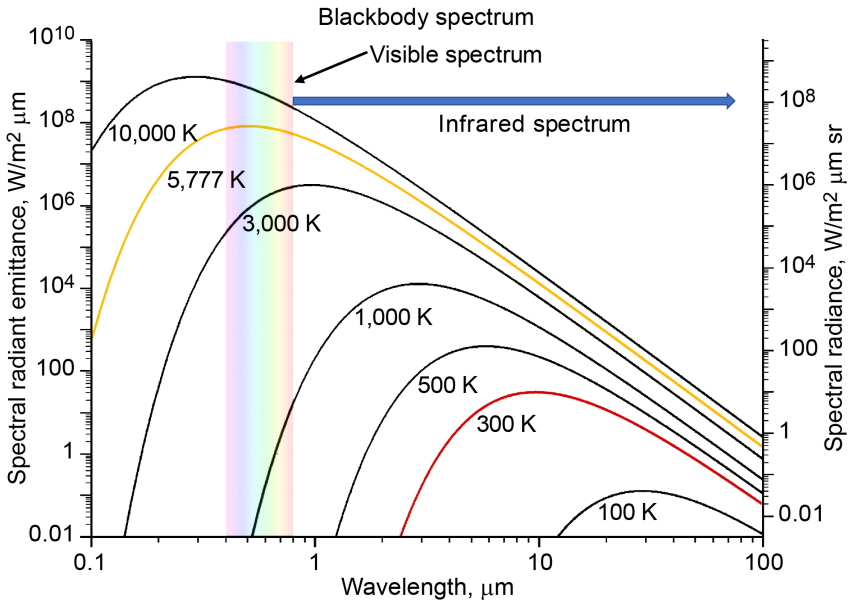

Figure 14.—Blackbody emission power per wavelength for various radiating temperatures (Ref. 33).

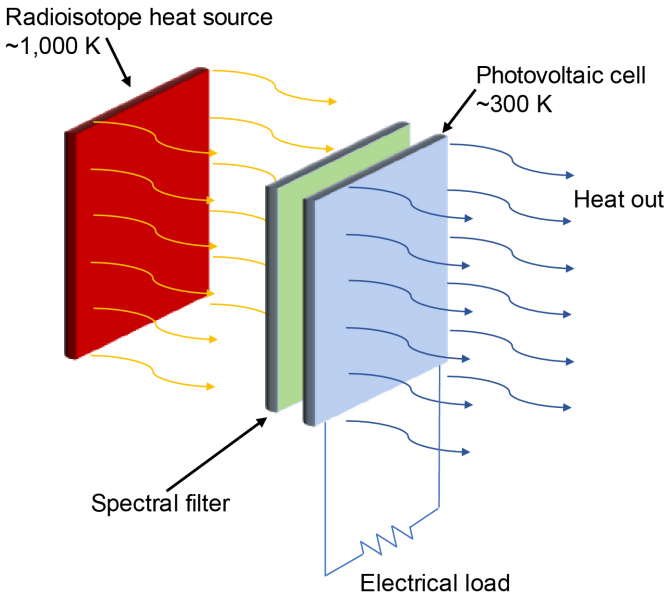

Figure 15.—Thermophotovoltaic operation.

To effectively collect power from the IR-emitting radioisotope, the TPV cells need to be tuned as close as possible to the peak of the emission spectrum. This requires the TPV system to be designed and insulated to operate at a specific temperature in order to maximize its power output. A spectrally selective filter is also used in enhancing the efficiency of the TPV cells by only transmitting the IR frequency that the cells are tuned to. The remaining IR radiation is reflected back to the heat source to help maintain its desired operating temperature (Ref. 32). This is illustrated in Figure 15.

A TPV power system would have the isotope heat source surrounded by the TPV cells. The back side of the cells would be cooled to keep their temperature at an acceptable level and reject the waste heat generated by the system. This arrangement is illustrated in Figure 16.

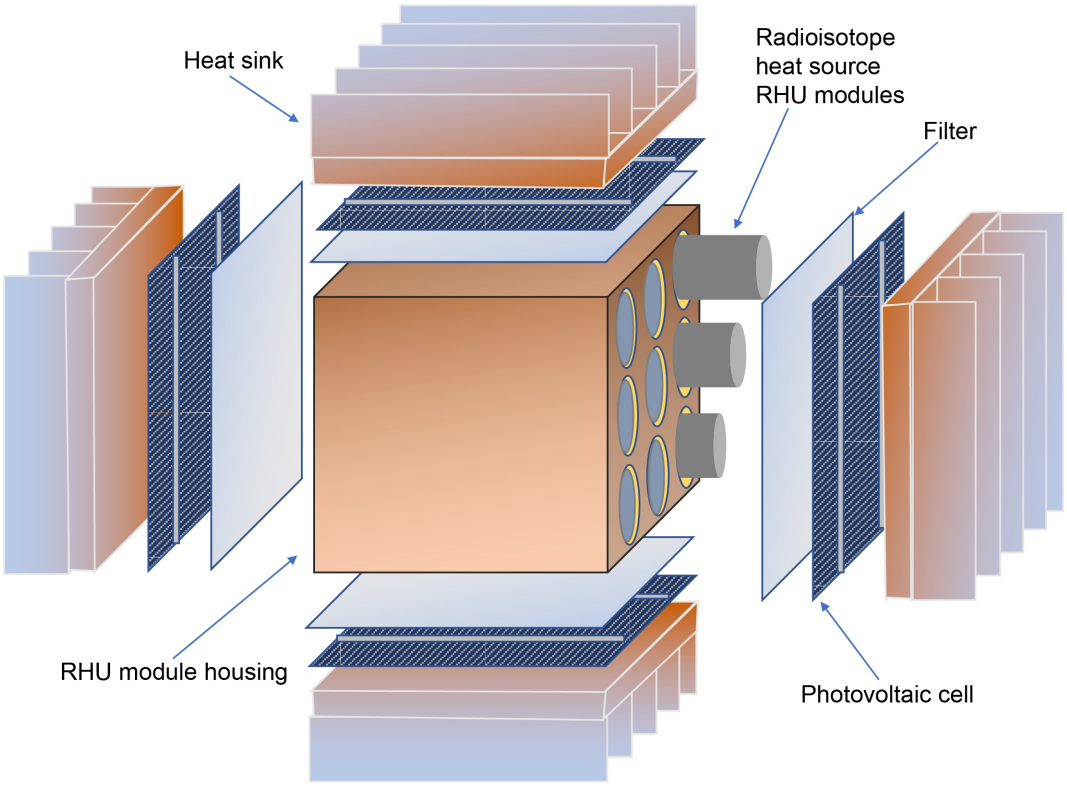

Figure 16.—Thermophotovoltaic power system. RHU, radioisotope heater unit.

The measured performance of components of a TPV system operating at just under 1,300 K produced an efficiency of just over 16 percent with projected efficiencies above 28 percent (Ref. 34). In other work, the estimated efficiency range for a TPV system with an AmO_2 isotope source was 5 to 9 percent with a heat source temperature of 980 and 1090 K, respectively (Ref. 35).

As with the thermionics, the main drawback to the TPV system is the need for a heat source that operates at high temperatures (in the 1,000 K range). For a small microwatt system, insulating a heat source so that those temperature levels can be achieved with small amounts of the radioisotope material can be problematic.

1.5.4 MicroStirling Radioisotope Heater Unit (RHU) Power System

Stirling cycle engines have been used in conjunction with radioisotope heat sources to produce power. This type of power source has been designed and extensively tested but has yet to be flown on a space mission. The most recent and extensively tested isotope-powered Stirling engine is the advanced Stirling radioisotope generator (ASRG). The ASRG utilized the general-purpose heat source (GPHS) as the heat source for the engine. A single GPHS block provides 250 W of heat and an ASRG system utilized two of these blocks. This power level is well beyond the low-output power levels identified from the other sources and the mass of ^{238}Pu isotope used in one GPHS block is orders of magnitude higher than the isotope mass considered for the low-output power applications. However, the Stirling engine system can be scaled down to lower power levels. It is conceivable to utilize a small Stirling engine with an RHU as the heat source to provide low-level electrical power. A Stirling engine could potentially operate off of one RHU with a projected hot end temperature of approximately 600 K and an output power of 105 mW (Ref. 36). This represents an efficiency of 10.5 percent.

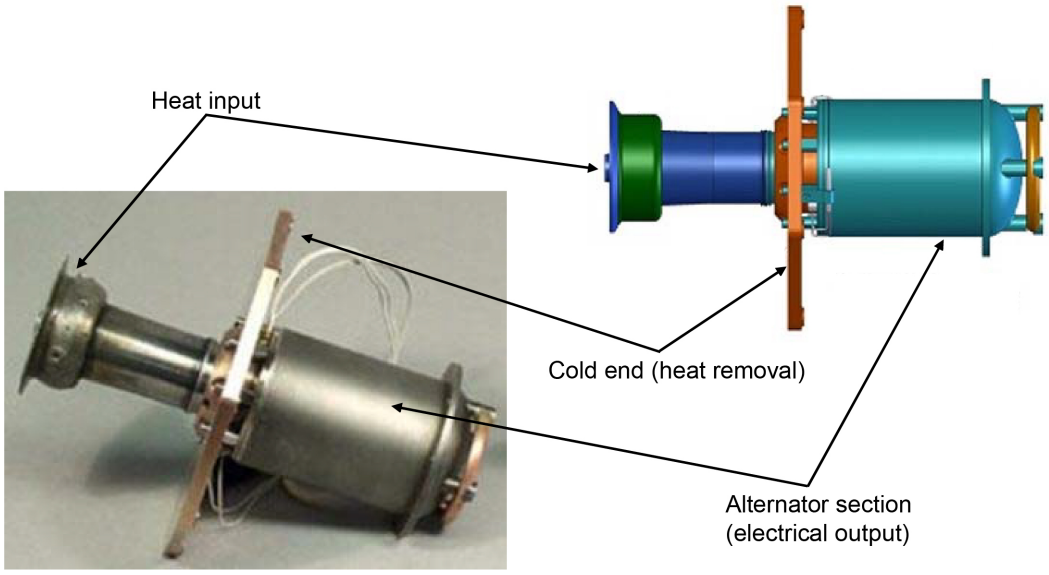

Figure 17.—Small-scale Stirling engine example (Ref. 37).

Small-scale Stirling engines have been produced for a number of applications. An example of a small scale Stirling cycle engine developed by NASA is shown in Figure 17.

Current work is underway at NASA Glenn Research Center on the development of an RHU-powered Stirling power converter for low-power space applications (Ref. 38).

1.6 Vacuum Collector

A vacuum collector power system operates in a fashion similar to a capacitor in which the alpha and beta particles charge plates. A vacuum is set up between the plates. The emitter plate or electrode is coated with a radioisotope that releases charged particles. The charged particles move toward the collector plate (electrode). This builds up a charge difference between the emitter and collector plates. A load connected between the two plates will complete the circuit producing current flow (Ref. 39). This is illustrated in Figure 18.

Although feasible, this approach has not been developed into an operational power system. This is mainly due to its projected low operating efficiency and the need to maintain a vacuum within the device. The other approaches are easier to construct, lighter weight, and operate at higher efficiency.

2.0 Isotope Material Dose and Mass Limits for Space Flight

There are limits placed on the amount or mass of a radioisotope that can be used in a spacecraft before special handling and procedures are required. This limit is determined by the activity limit values for a specific type of radioactive material, termed A1 and A2. These values are used to assess the transportability of radioactive material. Type A packaging can be used when the radioactivity of the material does not exceed the A1 or A2 values. Type A transportation encompasses normal transportation conditions and minor accidents. Radioactivity levels below the A1 and A2 values can be flown in spacecraft without any special handling. The goal of type A packaging is to prevent the loss or dispersal of the radioactive material and provide some basic levels of radiation shielding under normal transportation conditions and must withstand water spray, drop, puncture, and crash tests. If the radioactivity level of the isotope material used exceeds the A1 and A2 values, then type B or C packaging is required along with special handling. These types of packaging can withstand serious accidents such as spent nuclear fuel casks.

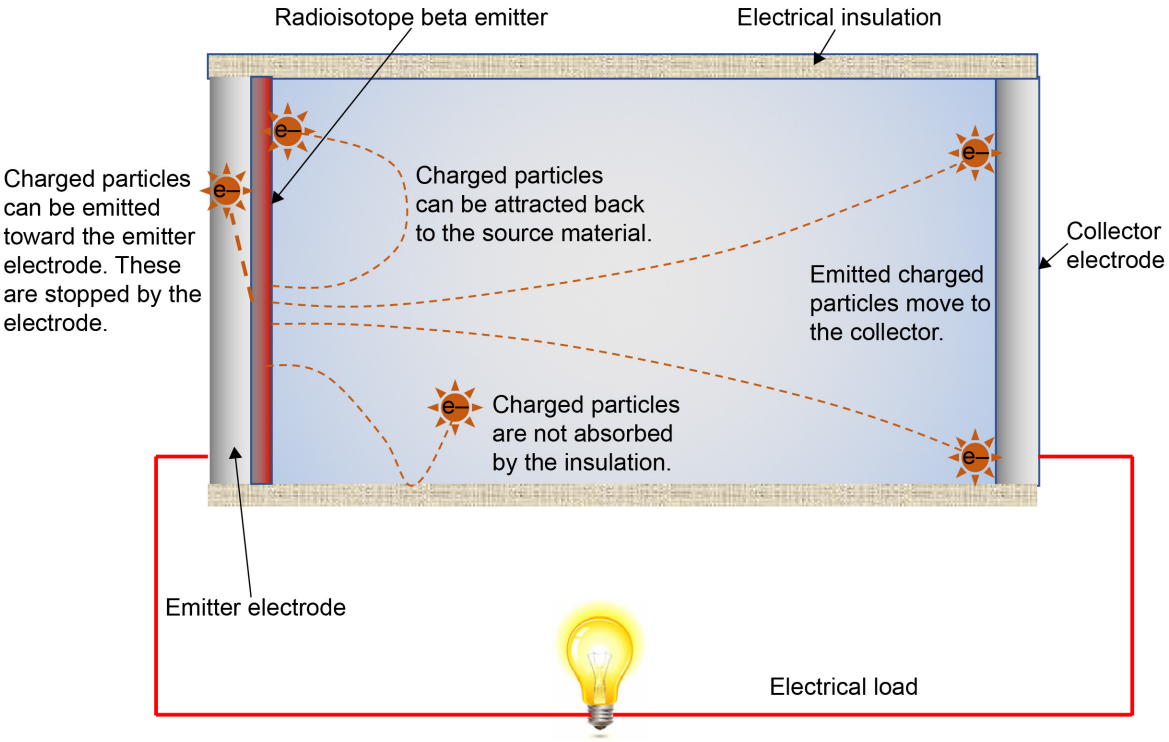

Figure 18.—Vacuum collector.

The activity limit A1 is for special form radioactive material such as an indispensable solid material or a sealed capsule containing the radioactive material. The A1 limit is determined by assuming that if an accident occurs, the sealed source or material block will be released, but there is no dispersal of its radioactive content. The A1 value is defined as the quantity of a radioactive material that will produce a gamma dose rate of 0.1 Sv/h or a beta dose rate of 1 Sv/h at a distance of 1 m from the sealed source material. For alpha emitters, the limit dose rate is 10,000*A2.

The activity limit A2 also relates to transportation accidents and hazards but with additional potential exposure pathways in the event the material is dispersed. These pathways include gamma exposure, beta radiation skin exposure, inhalation of radioactive material, ingestion, or radioactive material and gamma exposure from immersion in a gaseous cloud of the radioactive material. The first two of these pathways is also used in the A1 limit determination.

Based on these limits, an estimate of the amount of radioactive material that can be used onboard a spacecraft before special transportation and handling is required can be made. These limits for the isotopes given in Table II are listed in Table V. The values of A1 and A2 are given in Ci. They are also found listed as terabecquerel (TBq) where 1 Ci = 0.037 TBq (Refs. 40 to 42).

Table V also lists the total power that can be produced by the various isotopes. This power is the theoretical maximum for the A1 and A2 mass limits imposed by the packaging. The actual power produced will be less than this and is determined by multiplying this maximum power level by the efficiency of the power conversion technique used to produce an electrical output.

TABLE V.—ALLOWABLE RADIOISOTOPE MASS FOR A PACKAGING

Isotope	A1, Ci	A2, Ci	Specific activity, Ci/g	Allowable mass for A1 packaging, g	Allowable mass for A2 packaging, g	Max. power (100% efficient), W
^{3}H (tritium)	1,080.0	1,080.0	9,700.0	0.11	0.11	0.0357
^{22}Na	13.5	13.5	6,300.0	0.0021	.0021	.016
^{35}S	1,080.0	54.1	42,481.0	.025	.0012	1.08 .054
^{42}Ar	5.41	5.41	260.0	.002	.002	.0018
^{60}Co	10.8	10.8	1,100.0	.0098	.0098	.00565
^{63}Ni	1,080.0	811.0	57.0	18.95	14.23	.111 .084
^{85}Kr	541.0	270.0	390.0	1.39	.69	.809 .402
^{90}Sr	5.41	2.70	140.0	.04	.02	.0064 .0032
^{106}Ru	5.41	5.41	3,300.0	.0016	.0016	.000314
^{113}Cd	541.0	2.43	220.0	2.46	.011	.062 .00028
^{125}Sb	54.1	23.4	1,000.0	.054	.023	.0289 .0123
^{129}I	Unlimited	Unlimited	0.00018	No limit	No limit	.000157
^{137}Cs	54.1	13.5	87.0	.62	.16	.04994 .01289
^{147}Pm	1,080.0	24.3	930.0	1.16	.026	.396 .0887
^{151}Sm	1,080.0	108.0	26.0	41.54	4.15	.130 .013
^{155}Eu	541.0	54.1	490.0	1.10		.118 .0118
^{171}Tm	1,080.0	270.0	1,100.0	.98	.25	.159 .041
^{194}Os	5.41	5.41	310.0	.018	.018	.00317
^{204}Tl	108.0	13.5	460.0	.24	.03	.228 .029
^{210}Pb	16.2	0.243	76.0	.21	.003	.0016 2.3196×10^{-5}
^{227}Ac	1,080.0	.000541	72.0	15.0	7.5×10^{-6}	.0715 3.5734×10^{-8}
^{228}Th	811.0	.0108	820.0	.99	1.3×10^{-5}	.520 6.8338×10^{-6}
^{232}U	81.1	.00811	22.0	3.69	3.6×10^{-4}	2.55 .000249
^{238}Pu	54.1	.00541	17.0	3.18	3.182×10^{-4}	1.776 .000177
^{241}Pu	1,080.0	.270	100.0	10.8	.0027	.0346 8.6621×10^{-6}
^{243}Cm	81.8	.00811	50.0	1.62	.0002	3.00 .0003

3.0 Conclusions

The development of low-power isotope systems has been ongoing at a low level since the mid-20th century. A few of these devices have achieved commercial availability, mainly for military applications. However, research and development has continued in universities, government labs, and to a lesser extent in private companies. A summary of some of the low-power isotope systems that have been or are being developed and their potential efficiency and output power is listed in Table VI.

TABLE VI.—EXAMPLES OF LOW-POWER RADIOISOTOPE-BASED POWER SOURCE CURRENT DEVELOPMENT

Organization	Process	Isotope used	Max. output power	Status and/or notes
University of Missouri	Betavoltaics	^{35}S	687 nW	Lab prototype
University of Missouri	Water radiolysis betavoltaics	^{90}Sr	75.02 μW/cm^2	Lab prototype
Widetronix, Inc. (Ref. 43)[a]	Betavoltaics	TiH^3	5 nW to 1 μW	Engineering prototype and custom production
U.S. Army Research Laboratory	PIDEC[b]	^3H gas/ZnC:Cu	~100 μW	Lab prototype
City Labs, Inc.	Betavoltaics	^3H	1.4 to 5.6 μW	Commercially available
Betta Batteries, Inc.	Betavoltaics	^3H	100 μW	Experimental; under development
Donald W. Douglas Laboratories	Betavoltaics	^{147}Pm	400 μW	Made from 1968 to 1974
Cornell University	Betavoltaics	^{63}Ni	----------	SiC-B p-n junction material, under development
Qynergy	Betavoltaics	^{85}Kr	50 μW	Prototype development in conjunction with the Naval Surface Warfare Center Crane
Betta Batteries, Inc./University of Rochester	Betavoltaics	^3H	----------	Pre-prototype development
University of Missouri	PIDEC	^{85}Kr	----------	Pre-prototype development
NASA Glenn Research Center	RHU[c] Stirling	^{238}Pu	105 mW	Pre-prototype development
Massachusetts Institute of Technology	Radioisotope TPV[d]	^{238}Pu	----------	Simulation
General Atomics	Radioisotope TPV	^{238}Pu	1 mW to 10+ W	Simulation and pre-prototype development
BIAPOS	Thermoelectrics	^{238}Pu	426 mW	Prototype development
Hi-Z Technology/Jet Propulsion Laboratory	Thermoelectrics	^{238}Pu	40 mW	Prototype development
Lawrence Livermore National Laboratory	Betavoltaics	^{147}Pm	----------	Pre-prototype development

[a]Thomas, Christopher; Portnoff, Samuel; and Spencer, M.G.: High Efficiency 4H-SiC Betavoltaic Power Sources Using Tritium Radioisotopes. Appl. Phys. Lett., vol. 108, no. 1, 2016, p. 013505.
[b]Photon intermediate direct energy conversion.
[c]Radioisotope heater unit.
[d]Thermophotovoltaic.

References

1. Elder, J.T.; and Seidle, B.: Research and Development in Radioisotope Power Sources, and Applications Within the Navy, DoD and Other Agencies. Presented at the Isotope-Based Energy Sources Topical Meeting, Washington DC, 2017.
2. Sims, G.H.E.; and Juhnke, D.G.: The Beta Self-Absorption of Ni^{63} as Metallic Nickel. International Journal of Applied Radiation Isotopes, vol. 18, no. 10, 1967, pp. 727–728.
3. Epstein, J.; and Harris, D.: Properties of Selected Radioisotopes. A Bibliography Part I—Unclassified Literature. NASA SP–7031, 1968. http://ntrs.nasa.gov
4. Todd, G. Daniel: Toxicological Profile for Cobalt. Agency for Toxic Substances and Disease Registry Draft 205–1999–00024, 2001.
5. Schott, Robert J.: Photon Intermediate Direct Energy Conversion Using a Sr-90 Beta Source. Ph.D. Dissertation, Univ. of Missouri, 2012.
6. Shirwadkar, U., et al.: Enhanced Beta Batteries for Long Term Remote Applications. Presented at the Isotope-Based Energy Sources Topical Meeting, Washington DC, 2017.
7. Colle, R.: Primary Radioactivity Standardization of Ni-63. National Institute of Standards and Technology, Gaithersburg, MD, 2016.
8. Element Collection, Inc.: Periodic Table. http://periodictable.com. Accessed Aug. 7, 2018.
9. Luo, N.; Ulmen, B.; and Miley, George H.: Nanopore/Multilayer Isotope Batteries Using Radioisotopes From Nuclear Waste. University of Illinois, Chicago, IL, 2016.
10. Kim, Baek Hyun; and Kwon, Jae W.: Plasmon-Assisted Radiolytic Energy Conversion in Aqueous Solutions. Sci. Rep., vol. 4, Article 5249, 2014.
11. Prelas, M.A., et al.: A Two-Step Photon-Intermediate Technique for the Production of Electricity, Chemicals or Lasers in Nuclear Energy Conversion. Prog. Nucl. Energ., vol. 23, no. 3, 1990, pp. 223–240.
12. Prelas, Mark, et al.: Power Density Dilution Due to the Interface of the Isotope With the Transducer. Nuclear Batteries and Radioisotopes, Springer, New York, NY, 2016, pp. 177–220.
13. RMD: Gamma Scintillation Detector-Strontium Iodide (SrI_2). RMD Data Sheet, 2017.
14. Lin, Chia-Feng., et al.: InGaN-Based Solar Cells With a Tapered GaN Structure. J. Cryst. Growth, vol. 370, 2013, pp. 97–100.
15. Essig, Stephanie, et al.: Raising the One-Sun Conversion Efficiency of III-V/Si Solar Cells to 32.8% for Two Junctions and 35.9% for Three Junctions. Nat. Energy, vol. 2, no. 17144, 2017.
16. Panferov, Alexander; and Kurinec, Santosh K.: Modeling Quantum Efficiency of Ultraviolet 6H-SiC Photodiodes. IEEE Trans. Electron Devices, vol. 58, no. 11, 2011.
17. Collinson, A.J.L.; and Hill, R.: The Fluorescent Response of NaI(TI) and CsI(TI) to X Rays and γ Rays. Proc. Phys. Soc., vol. 81, 1963, p. 883.
18. Wang, Xiaojuan; and Gao, Mingyuan: A Facile Route for Preparing Rhabdophane Rare Earth Phosphate Nanorods. J. Mater. Chem., vol. 16, 2006.
19. Boutboul, T., et al.: An Improved Model for Ultraviolet and X-Ray-Induced Electron Emission From CsI. J. Appl. Phys., vol. 86, no. 10, 1999, pp. 5841–5849.
20. ThermoFisher Scientific: Fluorescent Probes. 2017. https://www.thermofisher.com/us/en/home.html Accessed Aug. 7, 2018.
21. Schreck, Matthias, et al.: Ion Bombardment Induced Buried Lateral Growth: The Key Mechanism for the Synthesis of Single Crystal Diamond Wafers. Sci. Rep., vol. 7, 2017, p. 44462.
22. Prelas, Mark A., et al.: A Review of Nuclear Batteries. Prog. Nucl. Energ., vol. 75, 2014, pp. 117–148.

23. Simoes, Raul, et al.: Diamond and Other Carbon Related Materials Applications in Photovoltaic Solar Cells. IEEE International Conference on Electro-Information Technology, Rapid City, SD, 2013.
24. Dalven, Richard: Temperature Coefficient of the Energy Gap of β-Silicon Carbide. Phys. Chem. Solids, vol. 26, 1965, pp. 439–447.
25. Levinshtein, Michael E.; Rumyantsev, Sergey L.; and Shur, Michael S., eds.: Properties of Advanced Semiconductor Materials GaN, AlN, SiC, InN, BN, SiC, SiGe. John Wiley & Sons, Inc., New York, NY, 2001, pp. 93–1.
26. O'Connor, J.R.; and Smiltens, J., eds.: Silicon Carbide: A High Temperature Semiconductor. Pergamon Press, Oxford, England, 1960, p. 366.
27. Heremans, Joseph P.: Thermoelectricity: The Ugly Duckling. Nature, vol. 508, 2014, pp. 327–328.
28. NASA Radioisotope Power Systems. https://solarsystem.nasa.gov/rps/rhu.cfm Accessed Aug. 7, 2018.
29. National Aeronautics and Space Administration: Improved Thermoelectric Converter Units and Power Generators. NASA Tech Brief, 1999.
30. Snyder, G.J., et al.: Testing of Milliwatt Power Source Components. IEEE Twenty-first International Conference on Thermoelectronics Proceedings, Long Beach, CA, 2002.
31. Stanford University: Stanford Nanoelectromechanical Systems, Thermionic Energy Conversion. https://nems.stanford.edu/thermionic-energy-conversion Accessed Aug. 7, 2018.
32. Multiscale Energy Laboratory. 2017. http://mel.khu.ac.kr/ Accessed Aug. 7, 2018.
33. Sun.org: Black Body Radiation. http://www.sun.org/encyclopedia/black-body-radiation Accessed Aug. 7, 2018.
34. Schock, A., et al.: Design, Analysis, and Optimization of a Radioisotope Thermophotovoltaic (RTPV) Generator, and Its Applicability to an Illustrative Space Mission. Acta Astronaut., vol. 37, 1995, pp. 21–57.
35. Goel, A., et al.: Design of a Flight Demonstration Experiment for Radioisotope Thermophotovoltaic (RTPV) Power System. Proceedings of Nuclear and Emerging Technologies for Space 2015 Conference, NETS Paper 5002, 2015.
36. Wilson, Scott D., et al.: Maturing Technologies for Stirling Space Power Generation. NASA/TM—2016-219415 (AIAA–2016–5017), 2016. http://ntrs.nasa.gov
37. Kontax Engineering Ltd.: Kontax Stirling Engines. http://www.stirlingengine.co.uk/HighTemperatureStirlingEngines/ Accessed Aug. 7, 2018.
38. Wilson, S.D., et al.: Radioisotope Heater Unit-Based Stirling Power Convertor Development at NASA Glenn Research Center. AIAA–2017–4715, 2017.
39. Miley, George H.: Direct Conversion of Nuclear Radiation Energy. American Nuclear Society, Hinsdale, IL, 1970.
40. North Dakota Department of Health Radiation Control: Table I A1 and A2 Values for Radionuclides. 2017. https://www.deq.nd.gov/publications/AQ/Radiation/FullRules/33-10-13.1.pdf
41. NASA General Safety Program Requirements. NASA NPR 8715.3C, 2008. https://nodis3.sfc.nasa.gov/
42. International Atomic Energy Agency: Regulations for the Safe Transport of Radioactive Material. Specific Safety Requirements No. SSR–6, 2012.
43. Thomas, Christopher; Portnoff, Samuel; and Spencer, M.G.: High Efficiency 4H-SiC Betavoltaic Power Sources Using Tritium Radioisotopes. Appl. Phys. Lett., vol. 108, no. 1, 2016, p. 013505.